



Construction and Properties of Sierpiński Triangular Fractals on Surfaces

Yifan Wang,^[a] Na Xue,^[a] Ruoning Li,^[a] Tianhao Wu,^[a] Na Li,^{*[a]} Shimin Hou,^{*[a]} and Yongfeng Wang^{*[a]}

Fractal structures are of fundamental importance in science, engineering, mathematics, and aesthetics. Construction of molecular fractals on surfaces can help to understand the formation mechanism of fractals and a series of achievements have been acquired in the preparation of molecular fractals. This review focuses on Sierpiński triangles (STs), representatives of various prototypical fractals, on surfaces. They are inves-

tigated by Monte Carlo simulations and ultra-high vacuum scanning tunneling microscopy. STs are bonded through halogen bonds, hydrogen bonds, metal-organic coordination bonds and covalent bonds. The coexistence of and competition between fractals and crystals are realized for a hydrogen-bonded system. Electronic properties of two types of STs are summarized.

1. Introduction

Fractals, with morphological features that fill the space in a non-integer dimension, exist extensively in nature, such as snowflakes, coastlines and leaves. As described by mathematician Mandelbrot, fractals with Hausdorff dimensions were "exactly the same at every scale or nearly the same at different scales".^[1] Understanding the mechanism of fractal growth is an issue of crucial importance for the potential application.

One of the ideal controllable systems for studying fractals is the molecular/atomic self-assembled structures. In 1915, the Polish mathematician Waclaw Sierpiński formulated an equilateral triangular fractal by connecting smaller equilateral triangles, which was considered as the origin of Sierpiński triangles (STs). Figure 1 shows a series of equilateral triangular structures, defined as ST-n for convenience, where n indicates the order of the molecular ST. As a typical representative of fractal structures, STs could be dated back to the 11th century in some decorative patterns and the earliest molecular scale STs in experimental systems were realized by means of the self-assembly of DNA tiles.^[2,3] Extensive computer simulations carried out on the fractals consisting of ST units verified the unique mechanical, electrical and magnetic properties of the STs.^[4]

In terms of experimental equipment, atomic resolution in real space is achieved by scanning tunneling microscopy (STM), which is now an established method for the research on self-assembly and growth processes. In the past 30 years, it has been amenable to study the surface molecular structure systematically by means of STM, providing a growing under-

standing of thermodynamics and kinetics of on-surface self-assembled structures.

As far as theoretical simulation concerned, the canonical lattice Monte Carlo simulation is a useful tool to investigate large molecular systems in variational conditions. Nieckarz and Szabelski presented a theoretical prediction of defect-free STs utilizing the simple molecular structures that was showed schematically in Figure 2.

They demonstrated that specific 120° backbone of the precursors was an essential criterion for the formation of molecular STs.^[5] The ratio of the linker molecules A to the metal atoms was set to three to two and the overlays of the simulation system were annealed for a more accurate result. Heterotactic (a) and homotactic (b) three-fold coordination nodes stabilizing the metal-A aggregates are shown in Figure 3. Among the mixtures, only heterotactic nodes (a) could form

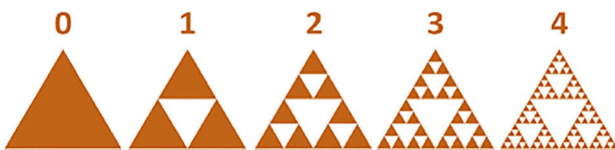


Figure 1. Models of the Sierpiński triangles.

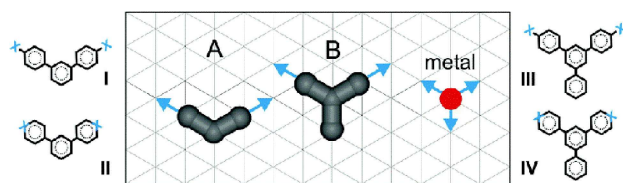


Figure 2. Schematic structure of exemplary linker molecules with two (120°) electron donor centers (X) and their model counterparts A (I, II) and B (III, IV) used in the simulations on a triangular lattice. The blue arrows next to A and B indicate the directional metal-linker interactions while the arrows pointing outward the metal atom(red) show the attachment points accessible to the linker in a three-fold coordination node. Reproduced with permission from Ref. [5]. Copyright (2014) The Royal Society of Chemistry.

[a] Dr. Y. Wang, N. Xue, R. Li, T. Wu, N. Li, Prof. S. Hou, Y. Wang

School of Electronics Engineering and Computer Science

Peking University

No. 5, Yiheyuan Road, Haidian District, Beijing, 100871, China

E-mail: na-li07@pku.edu.cn

smhou@pku.edu.cn

yongfengwang@pku.edu.cn

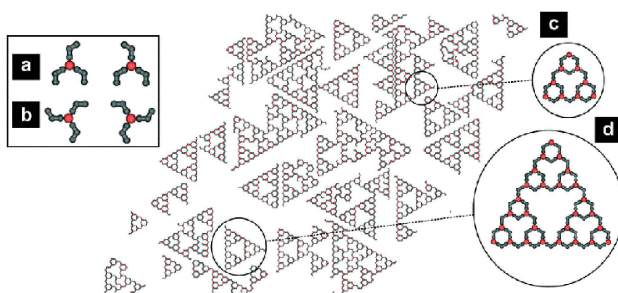


Figure 3. Representative snapshot of the adsorbed overlayer comprising 1800 molecules of A and 1200 metal atoms. Heterotactic (a) and homotactic (b) three-fold coordination nodes stabilizing the metal-A aggregates. Magnified fragments of the overlayer corresponding to the first (c) and second (d) generation of the Sierpiński triangle. Reproduced with permission from Ref. [5]. Copyright (2014) The Royal Society of Chemistry.

perfect STs, which were easily identified. The simulation demonstrated that the formation of STs was kinetically controlled.^[5] The ratio between three-fold heterotactic and homotactic nodes is 3 to 1. Their aggregation led to STs and two-dimensional crystals, respectively. The entropic stabilization of heterotactic nodes determined that the linker molecules preferred to form STs on surfaces. The reason for the absence of bigger triangular units in the simulation was related to the mechanism of fractal growth. Inactive perimeter of the fractal triangle increased and the number of vertices which played an active part in attaching the liner molecule to metal atoms was unchanged.

As for the synthetic strategy of the STs, recently, by designing a series of functional organic molecules with specific configuration as precursors, halogen bond,^[6] hydrogen bond,^[7] metal-organic coordination bond^[8–11] or covalent bond^[12,13] can be used as driving forces to prepare ordered Sierpiński triangle fractals on different surfaces. Figure 4 summarizes the precur-

sors on the basis of above theoretical simulations and extensive related experiments.

2. On-Surface Construction of ST Fractals

As mentioned above, molecular ST fractals can be constructed on surfaces. Figure 5 shows the reported methods of the on-surface preparation of the STs.

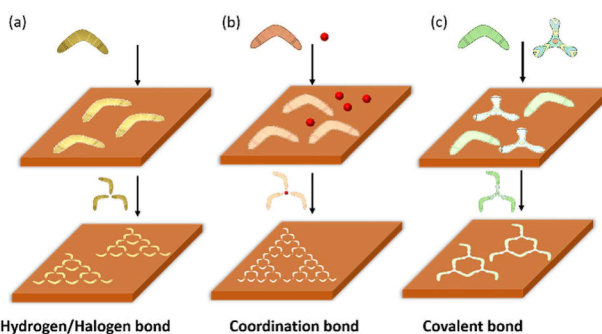


Figure 5. Schematic diagram of three methods for preparing molecular Sierpiński triangle fractals on surface through: a) halogen bonding or hydrogen bonding using a V-shape molecule, b) coordination bonding using a V-shape molecule, and c) covalent bonding using a V-shape and Y-shape molecules.

Owing to their geometrical characteristics, the V-shape molecules could be used to prepare STs through weak intermolecular interactions and stabilized at liquid nitrogen temperature (Figure 5a). STs stabilized at room temperature were successfully constructed based on coordination interactions between the V-shaped molecules and metal atoms as shown in Figure 5b. High-temperature stable STs were fabri-

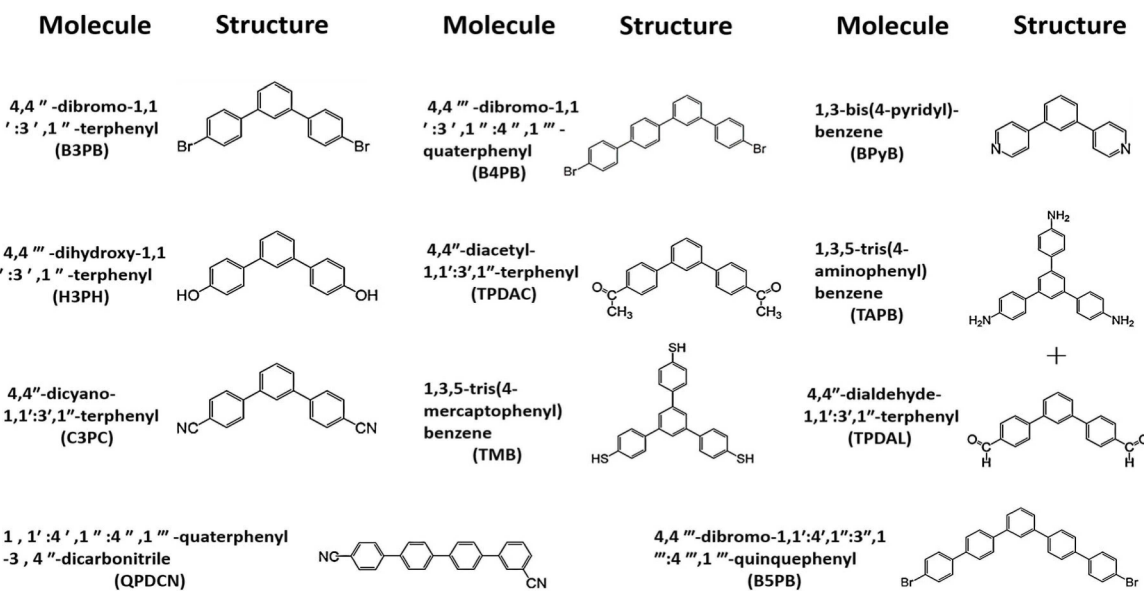


Figure 4. Typical molecules used as achiral precursors to form STs whose configuration is V-shaped, linear-shaped or star-shaped.

cated by covalent reactions between the V-shape and the 3-fold Y-shape molecules as shown in Figure 5c.

Shang J et al. reported the formation of extended and defect-free Sierpiński triangular fractals under the ultrahigh vacuum conditions for the first time.^[6] In their experiment, 4,4''-dibromo-1,1':3',1''-terphenyl (B3PB) and 4,4''-dibromo-1,1':3',1''-4'',1'''-quaterphenyl (B4PB) as the basic building blocks were used to prepare a series of planar molecular STs on Ag(111). The synergistic halogen and hydrogen bonds in these molecules played the role of driving force in the assembly. However, for the weak interactions in halogen bonds or hydrogen bonds, those fractals were quite unstable and only observed below the liquid-nitrogen temperature.

Metal–ligand interactions are generally stronger than halogen bonds or hydrogen bonds and thus can form more robust entities. Moreover, the incorporation of metal centers increases the scope of the functional properties of the fractal structures and allows us to design strategies based on metal-directed assembly.^[14,15] Xu Wei's group synthesized a 120° ditopic organic molecule with carbonitrile end groups capable of coordinating with nickel atoms. They have constructed the metal–organic Sierpiński triangles on Au(111) via on-surface coordination chemistry successfully.^[8] Besides, our group have also prepared the STs up to third-order on the Au(111) surface by the coordination of 4,4''-dicyano-1,1':3',1''-terphenyl(C3PC) organic molecules and metallic iron (Fe).^[9]

Covalently bonded second-order STs were prepared at vacuum-solid interfaces by Schiff-base reaction of 4,4''-dialdehyde-1,1':3',1''-terphenyl (TPDAL) and 1,3,5-tris(4-aminophenyl) benzene (TAPB) on Au(111) for the first time.^[12] The STs prepared in this experiment could persist at 500 K, indicating better thermal stability of the covalently bonded STs than other fractals. However, the second-order Sierpiński triangles was the largest fractals observed in this experiment. Combining with theoretical calculations, we inferred that the irreversibility of the covalent reaction and inadequate migration of molecules were the key factors limiting the growth of covalent fractal structures. Remarkably, three-order covalently bonded Sierpiński triangles have been formed by Markus Lackinger et al.^[13] The STs emerged after annealing the molecular chain structure assembled by 1,3,5-tris(4-mercaptophenyl) benzene (TMB) and Au atoms via S–Au–S bond. The formation of the STs was driven by the transformation of coordinative Au-thiolate to covalent thioether linkages. In this work, initial coordinative S–Au–S bond stabilized the precursor molecules on Au(111) effectively. With the further increase of reaction temperature, free Au atoms facilitated the dissociation of C–S bonds and covalent C–S–C bonds with angle of 120° formed.^[13] Recent progresses about the construction and properties of STs would be discussed in details below.

2.1. Coexistence and Competition between 1.6-Dimensional Fractal and 2-Dimensional Crystal

The STs and 2D molecular crystals could be formed by V-shape 4,4''-ihydroxy-1,1':3',1''-terphenyl (H3PH) molecules with –OH

groups on both ends.^[7] After sublimating H3PH molecules to Au(111) substrate kept at room temperature, discrete cyclic hydrogen bonded STs were formed at low coverages.

Figure 6 shows STM images and DFT-optimized structures of STs with order from 0 to 3. The Monte Carlo simulation indicated that the entropic stabilization of heterotactic H3PH trimers played a key role in the formation of STs. Besides the STs, quasi-one-dimensional (1D) chains and 2D crystals coexisted on Au(111) as shown in Figure 7a at a higher molecular coverage. These periodic chains in Figure 7b were built of heterotactic tetramers whose schematic structure was showed in Figure 7d. The finite width of the face-centered-cubic (fcc) region of the Au(111) surface limited the further lateral expansion of the one-dimensional supramolecular chain.

By altering surface coverage, we characterized the competition between the ST fractals and the crystalline phase. According to the results summarized in Figure 7f, we concluded that the H3PH molecules self-assembled mainly into the STs and a few chain structures at a low coverage. The ordered 2D crystals formed and dominated the substrate ultimately with a higher coverage and the reverse transformation of the 2D crystal to the 1.6D fractal could be achieved by high-temperature annealing at a high coverage. The transformation between non-integer-dimensional fractals and integer-dimen-

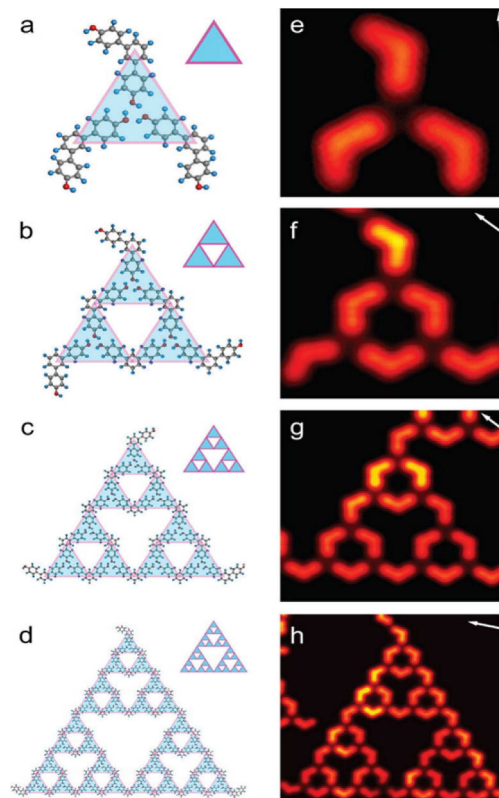


Figure 6. a–d) DFT-optimized molecular structure models of the STs sustained by the cyclic O...H–O hydrogen bonds. e–h) Constant height STM image of the adsorbed molecular configuration corresponding to (a–d) on Au(111) obtained at 100 mV. Reproduced with permission from Ref. [7]. Copyright (2015) American Chemical Society

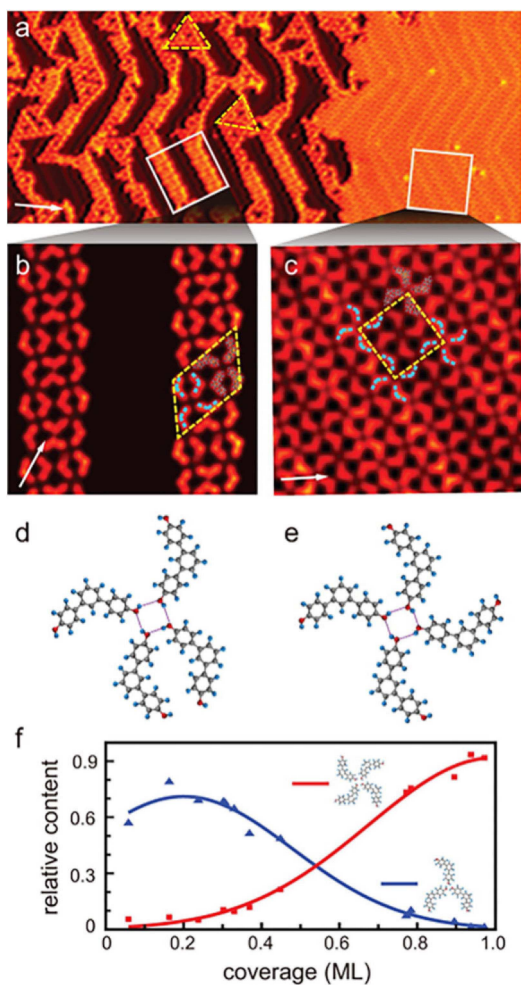


Figure 7. a) Quasi-one-dimensional molecular chain, a two-dimensional crystal phase and a 1.6-dimensional triangular fractal coexist on Au(111). STs marked by yellow dotted triangle. b) STM image of Quasi-one-dimensional molecular chain. c) STM image of two-dimensional crystal structure. d–e) DFT-optimized heterotactic and homotactic tetrameric units. f) Effect of surface coverage on the relative amount of the trimer forming fractal phase and the tetramer which account for crystal phase. Reproduced with permission from Ref. [7]. Copyright (2015) American Chemical Society.

sional crystals is very complex and yet intriguing, which might help to understand the forming mechanism of STs.

2.2. From Isolated Fractals to Ordered Fractal Arrays

Constructing STs with higher orders or packing them into crystalline structures can serve as an efficient and versatile way to experimentally prove the magnetic, mechanical, or optical properties of the STs.^[17,18]

However, the random nucleation center always forms during STs growth, which makes the reported STs are either isolated or connect into a disordered network. So appropriate external restraint is an essential term to guide the isolated or disordered fractal units to form into ordered arrays. “Substrate template method”^[19–22] is of great application potential in either

atomic / molecular assembly^[23] or chemical synthesis,^[24] which is seen as a well-established method for constructing ordered fractal arrays. 1D double chains and 2D small domains of STs were successfully prepared taking advantage of the confinement of the template in this work.^[11] We defined 1D structure as a double-chain of ST-n triangles, or DCT-n for convenience in the following sections. The reconstructed surface of Au(100) had a ridge-like structure with periodic arrangement, and the reconstruction direction was along the [011] crystal orientation. Reconstructed Au(100) surface as a substrate template is widely used in the field of surface physics chemistry.^[25,26] By sublimating the C3PC molecules on the reconstructed Au(100) surface with a certain coverage and subsequent deposition of Co atoms, metal-organic coordinating STs were obtained after annealing. Figure 8b and 8d display the molecular structure models corresponding to Figure 8a and 8c. The blue dotted lines in Figure 8d indicated the position of the reconstructed ridges where the periodic distance between adjacent green lines was 1.44 nm. From the images we could see the position of Co atoms was slightly higher than reconstructed rows in the upper ST, however, in the lower ST, the Co atoms were below them. The straight-line distance of Co in these two positions was 1.69 nm which was marked by red lines in Figure 8d. Figure 8e shows the longest chain structure observed in the experiment with the length up to 100 nm. Figure 8f is a schematic diagram of the self-assembly process of the chain structure.

In brief, our work described the entire evolution from the initial coordination between the molecules and metal atoms to the final formation of ordered one-dimensional fractal ribbons. The hierarchically assembled ordered DCTs could attribute to the template effect of the reconstructed Au(100)-(hex) substrate. Our results provided ideas and methods for preparing

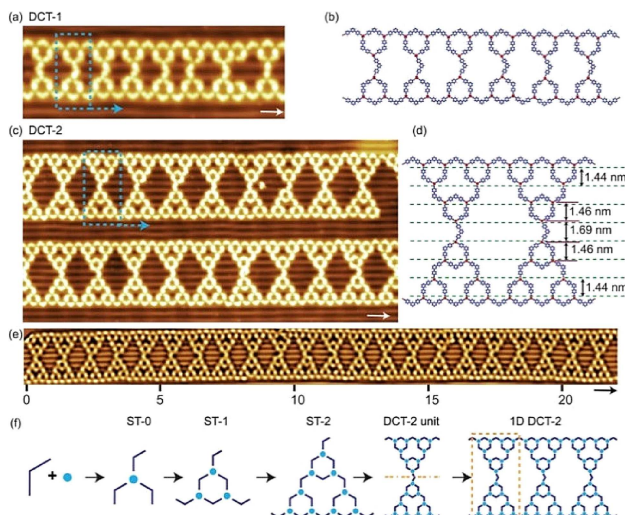


Figure 8. a–d) STM images and models of DCT-1 and DCT-2 . e) The longest DCT-2, which includes 22 repeating units. f) Schematic diagram of the self-assembly process of triangular fractal arrays. The white arrows in STM images indicate the [011] direction. Reproduced with permission from Ref. [11]. Copyright (2017) The Royal Society of Chemistry.

large-scale ordered fractal arrays, which are particularly instructive.

2.3. Cross-Step Growth Regardless of the Restriction of Surface Symmetry

The orientation of the molecules on the surface is significantly affected by the orientation of the substrate lattice. On account of the symmetry match between overall ST structures and substrate lattices, (111) surfaces are preferred choice for high order STs. High-order STs are usually prepared on the inert Au(111) and Ag(111) surfaces, where the molecule-molecule interaction plays a more important role in the formation of surface structures. On more reactive substrates, the molecule-substrate interactions dominate the molecular assembled structures and three-fold symmetric nodes, which are prerequisites for the formation of STs, cannot be prepared in a controlled way. This explains why high-order STs are not formed on Cu(111).

Previous studies have manifested that hydroxyl groups ($-OH$) could form three-fold Fe–O bonds on surfaces with Fe atoms.^[27] Such robust bonds were conducive to fabricate STs on non-three-fold substrates. After co-depositing hydroxyl terminated V-shaped molecule H3PH and Fe atoms on Ag(100), the defect-free Fe–O coordinated STs formed on this symmetry-mismatched fourfold surface through chemical reaction, which broke the restriction of surface symmetry.^[10] Figure 9a shows three Fe-STs-3 crossed a step. Figure 9b is more evident after a Laplace transformation on the basis of Figure 9a. On a symmetry mismatched substrate, the molecules at the edge of the steps needed to re-adjust their orientation to better fit the topography of the steps (see the yellow dotted circle). Here, the strong Fe–O bonds were sufficient to ensure that the growth of STs was not disturbed by reorientation of H3PH molecules on the edge.

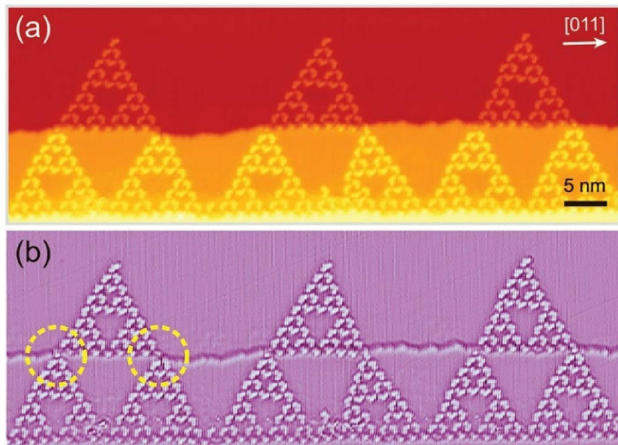


Figure 9. STM image of Fe-STs-3 crossing a step on Ag(100) a) before and b) after the Laplace transformation of (a). Reproduced with permission from Ref. [10]. Copyright (2016) The Royal Society of Chemistry

The cross-step H3PH molecules linked the STs on two terraces, constructing a ST of higher order. DFT calculations were performed to quantify the intensity of the Fe–O interaction in the STs. Metal-organic coordination had higher strength and flexibility than hydrogen bonding or halogen bonding. Hence, Fe–O coordination STs could remain consecutive while crossing the surface steps.

2.4. Preparation of High-Order STs by Combining Templating and Co-Assembly Methods

The highest order of the STs prepared previously by various methods was only 4 and it had been impossible to break the limitation of the kinetic growth when trying multifarious experimental conditions. Our group proposed an effective way to prepare STs up to fifth order with a lateral length of 0.05 μ m on the reconstructed Au(100)-(hex) substrate by combining the templating and co-assembly methods.^[28] The templating method plays a role in taking tangible shape of nucleation centers and co-assembly method^[29,30] accounts for the sequential formation of STs.

In this experiment, we deposited C3PC molecules and Fe atoms on the substrate at room temperature. 1D double chains constructed by metal-organic coordinating STs emerged. Interestingly, when BPyB molecules replaced 13–26% of C3PC molecules, the chain structure disappeared and complete fifth-order STs formed under the effect of co-assembly. We found that the fifth-order STs were obtained in the circumstantial conditions where the ratio of metal to linker exceeded 2:3 and the ratio of C3PC to BPyB was about 3:1. Figure 10 shows STM images of a series of C3PC-BPyB-Fe-ST-n with n equal to 0–5 and their corresponding models of STs.

In addition, we separately studied the adsorption assembly of C3PC and Fe atoms on Au(100). A series of one-dimensional double-chain structures composed of ST-2 were formed after annealing for 5 minutes and densely packed along the [011] direction of the substrate. The emergence of ordered double-chain structures rather than fractals resulted of template effect of the reconstructed Au(100)-(hex) substrate. When BPyB molecules and Fe atoms were co-deposited on Au(100), three order STs formed via the coordination between N–Fe.

Furthermore, we proposed a possible mechanism of the formation of high-order STs. As shown in Figure 11, the green dashed line represents the reconstructed ridges of Au(100). If a BPyB molecule replaced the bridged C3PC molecule, it could

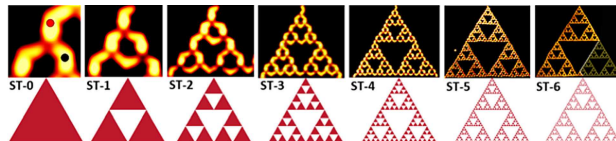


Figure 10. STM image of the high-order Sierpiński triangular fractal structure on the Au(100) surface. C3PC and BPyB are marked by red and black dots, respectively. Reproduced with permission from Ref. [28]. Copyright 2017, American Chemical Society

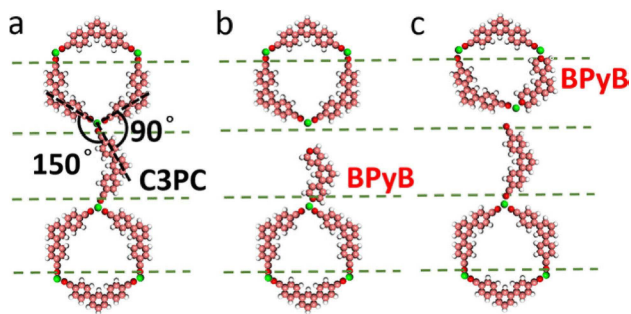


Figure 11. (a) Molecular and atomic model of the central structure of double chains. (b, c) Model in (a) with the bridged C3PC (b) or its neighboring molecule (c) replaced with a BPyB molecule. Reproduced with permission from Ref. [28]. Copyright (2017), American Chemical Society.

only bind to one Fe atom because of its short length. In this case, the chain got unstable and might form high-order STs. The similar transition happened if one of the four adjacent C3PC molecules around the bridged molecule was replaced by a BPyB molecule.

In short, the method put forward above provided a feasible approach to a promisingly vast range of functional high order Sierpiński triangles.

2.5. Formation of Fractals in Presence of Other Molecules

In the previous study, perfect triangular fractals have been prepared on various substrates under ultra-high vacuum. In light of expanding the potential application of fractals, we made every endeavor to construct STs in more complicated environments with the coexistence of other molecules.^[31] Molecular models of manganese phthalocyanine (MnPc) and Fullerene (C_{60}) molecule were showed in Figure 12a and 12d.

Certain STs formed after depositing C3PC molecules and Co atoms on the substrate. Co atom was invisible in the STM image for its stronger adsorption capacity and longer distance from the tip during imaging.^[32] To investigate the stability of the fractal structures under the influence of the C_{60} molecule, we annealed the sample for 10 minutes at different temperatures. A distinct disordered structure was observed as shown in Figure 12b after annealing the system at 400 K, on which C_{60} molecules were pre-deposited. With a series of statistics and data analysis, we concluded that the free diffusion of C3PC and Co on the substrate was impeded by the interference of C_{60} molecules. Three-fold nodes, as a prerequisite for fractal formation, were disrupted or became considerably more difficult to generate and maintain. However, by further annealing at 360 K, perfect high order STs were regained thanks to the weaker diffusion of C_{60} molecules, as shown in Figure 12c.

Because of the intermolecular dipole repulsion, MnPc molecules distributed separately on the Au(111) substrate.^[33] As shown in Figure 12e, reducing the coverage of C3PC molecules by annealing at 410 K, which resulted in the appearance of

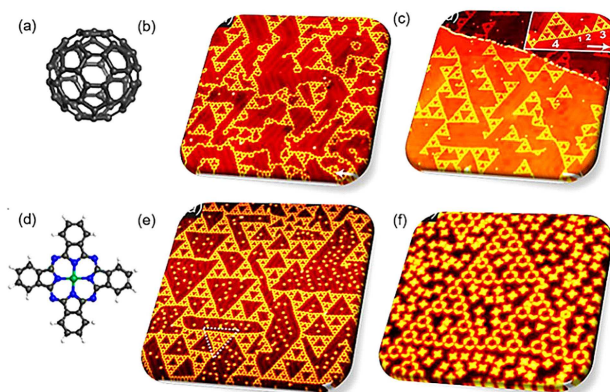


Figure 12. a,d) Molecular models of MnPc and C_{60} molecules. b) Large-scale STM image obtained after annealing the C_{60} deposited structure t 400 K for 10 min. c) STM image obtained after further annealing the sample at 360 K for 10 min. The inset shows STs from the first to fourth order. e) Large-scale STM image obtained after annealing the MnPc, C3PC and Fe atoms co-deposited structure at 400 K for 10 min. f) STs prepared with the coexistence of MnPc molecules at 0.25 ML. Reproduced with permission from Ref. [31]. Copyright (2017) The Royal Society of Chemistry.

higher order fractals. It demonstrated that the free diffusion of MnPc molecules barely influenced the high order STs formation. STs could survive even at a rather high coverage of MnPc, which was showed in Figure 12f.

From the fact that fourth-order metal-organic STs could be produced by C3PC molecules and Fe or Co atoms with the coexistence of C_{60} or MnPc molecules on Au(111), we came to a conclusion that neither C_{60} nor MnPc affected the formation of high-order STs. To be noted, the fractal structures disrupted by C_{60} molecules could be restored via low temperature annealing. And the MnPc molecules adsorbed selectively at certain holes of STs.

3. Electronic Properties in a Fractal Geometry

Previous research has indicated that it is the dimensionality that determines various properties of an electronic quantum system.^[34–36] For instance, electrons tend to present Luttinger liquid state in 1D, but show the quantum Hall effect in the case of 2D. Nevertheless, scientific studies, about characterization of electrons in non-integer, or fractional dimensions, are scant. Understanding the interaction between fractals and electrons is crucial to prepare novel electronic devices that aim to satisfy the growing demand for miniaturization and functionalization.

3.1. On-Surface Electronic Confinement Effects of Triangular Fractals

Crommie et al. constructed a quantum corral and visualized a clear standing wave pattern for the first time by positioning Fe atoms into a circular on Cu(111). This work was acknowledged as a classic artificial 2D electronic confinement system.^[37] More interestingly, STs, because of its unique configuration, provide

an alternative type of quantum corrals in comparison with 0D, 1D, and 2D resonators previously reported,^[38–45] which greatly promotes the research of quantum confinement effect. In order to study surface electronic states in triangular cavities, we used 120° V-shaped H3PH molecules and Fe atoms to fabricate defect-free STs up to fourth order on Ag(111).^[46]

In the series of constant-high differential conductance images (dI/dV mapping) as shown in Figure 13, it was clear that the number of alternating light and dark nodes of standing waves in the largest three-order cavities increased as the sample bias gradually increased from –30 mV. Figure 13b–d obtained at lower bias voltages reflected the shape of the wave function of the electronic ground level. At higher bias voltages, dI/dV maps corresponding to Figure 13e–h contained contributions from even more energy levels.

In a word, a standing wave pattern changing with the applied bias voltage was observed in the well-defined triangular quantum corrals which were prepared by H3PH molecules and Fe on Ag(111). And the larger the bias voltage was, the more standing wave nodes could be observed. What's more, the density of electron local states at different locations of various triangles were discussed in more detail in this work. Based on the two-dimensional scattering model, we qualitatively explained how the position and width of the standing wave resonance were affected by the size of the triangular cavities and the applied bias voltage, demonstrating that the elastic loss boundary scattering was the predominating broadening mechanism of the confined states in these ST corrals.

3.2. Artificial Creation of Electronic Quantum Fractals

The STs constructed by organic molecules are able to confine the on-surface 2D electron gas, which confirms the fractal

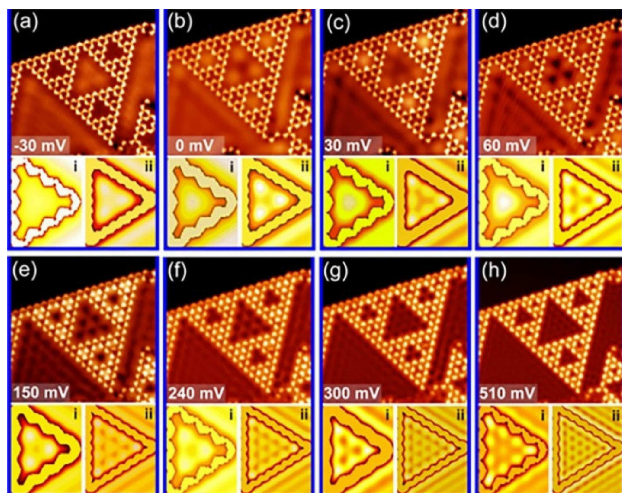


Figure 13. Upper part: The constant-high differential conductance images measured under different sample biases. Lower part: the corresponding simulated results obtained with the improved 2D multiple scattering model. i and ii represent the standing-wave patterns within the medium cavity and the largest one respectively. Reproduced with permission from Ref. [46]. Copyright (2018) American Physical Society.

structures can be used for the study of surface electronic properties. Recently, S. N. Kempkes et al. have manipulated CO molecules on Cu(111) to form a three-order electronic Sierpiński fractals for the first time.^[44] One of the highlights of this work was that the electron wave functions in the artificial Sierpiński triangle inherited the scaling properties of the Sierpiński geometry. The artificially constructed geometric, electronic fractals were denoted by G(n) and n was in the range of 1 to 3 in their work.

Figure 14 presents the wave function maps of artificial electronic Sierpiński triangular fractal structures including experimentally obtained dI/dV maps (left column), calculated LDOS maps using tight-binding model (middle column) and Muffin-tin approximation (right column), respectively. The red (R), green (G), blue (B) circles in the figure marked the three non-equivalent adsorption sites of the Sierpiński triangles. When $V = -0.325$ V, high LDOS was observed at the R, G and B sites, as well as in the areas in-between. This indicated that the wave function had strong bonding characteristics and thus generated strong conductivity along the path (R-B-G-B-R). At a bias voltage of –0.2 V, the overall wave function was split into nine parts due to the lower amplitude at the red position,

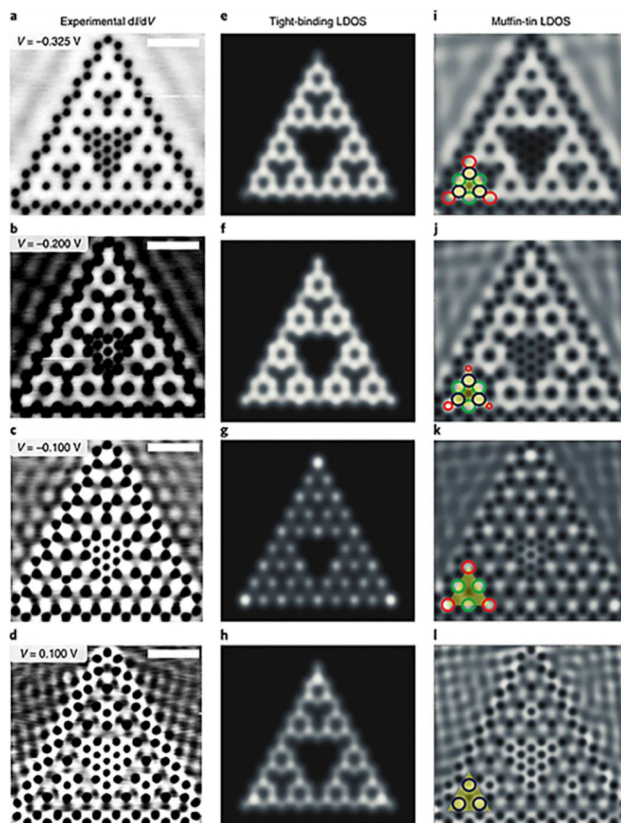


Figure 14. a–d) Differential conductance maps acquired above a G(3) Sierpiński triangle at bias voltages –0.325 V, –0.200 V, –0.100 V and +0.100 V. e–h) LDOS maps at these energies calculated using the tight-binding model. i–l) LDOS maps simulated using the muffin-tin approximation. G(1) building block is indicated, in which a larger radius of the circles corresponds to a larger LDOS at an atomic site, whereas no circle indicates a node in the LDOS. Reproduced with permission from Ref. [47]. Copyright (2018) Springer Nature.

corresponding to the first-order STs. A fully bonded wave function that appeared as integrally connected at -0.325 V , was divided into nine independent parts at -0.2 V , demonstrating the self-similarity of LDOS in the fractal structure. Furthermore, they found that the LDOS showed a dip on the blue sites and a peak at the green and red sites at $V = -0.1\text{ V}$. In virtue of the tight-binding calculation, they came to a conclusion that the nodes of wave function on the blue sites reflected a non-bonding molecular orbital from a chemical perspective. It was clearly recognized that electron conductivity along the path (R-B-G-B-R) affected by nearest-neighbor hopping had disappeared. Instead, electrons began to perform next-nearest neighbor hopping between the red and green sites. Finally, at $\pm 0.1\text{ V}$, all blue sites had high amplitudes, by contrast, red and green sites manifested lower amplitudes. And the box-counting method was used here to confirm whether the electronic wavefunctions inside the Sierpiński structure inherited the dimension of the geometric structure. The box-counting dimension of the Sierpiński triangle approximated the Hausdorff dimension. These results showed that the features of electronic wavefunctions in the artificial fractal also possessed the characteristics of fractal dimension. This work provided insight into future approaches to address the effects of spin-orbit interactions and magnetic fields on electrons in fractional dimensions.

4. Outlook

Fractals are not only of fundamental importance. They could be used in many areas such as electrical storage,^[48] stretchable electronics^[49] and plasmon.^[50] Typical examples of fractals are Cantor sets, STs, Sierpiński carpet, Dragon curves, Menger universal curves, Space filling curves, Koch curves. Up to now, only Sierpiński fractals can be prepared on surfaces in a controlled way. Recent theoretical studies show that Sierpiński carpet and gasket host topologically protected states when a perpendicular magnetic field is applied.^[51] In terms of STs, most researches are about the preparation methods. Further studies about their properties and applications are suggested. For example, there are holes of different size in STs, which might be used for gas adsorption and separation. Meanwhile, other types of fractals could be prepared on surfaces through molecular self-assembly, single-molecule manipulation^[47] and DNA nanotechnology.^[52]

Acknowledgements

This work is supported by the Ministry of Science and Technology (2018YFA0306003, 2017YFA0204702) and National Natural Science Foundation of China (21433011, 61621061).

Conflict of Interest

The authors declare no conflict of interest.

Keywords: fractals · scanning tunnelling microscopy · Sierpiński triangle · surface science · surface self-assembly

- [1] B. B. Mandelbrot, *The Fractal Geometry of Nature*, WH Freeman, 1982.
- [2] K. G. Libbrecht, *Rep. Prog. Phys.* **2005**, *68*, 855–895.
- [3] H. Brune, C. Romainczyk, H. Röder, K. Kern, *Nature* **1994**, *369*, 469–471.
- [4] E. van Veen, S. Yuan, M. I. Katnelson, *Phys. Rev. B* **2016**, *93*, 115428.
- [5] D. Nieckarz, P. Szabelski, *Chem. Commun.* **2014**, *50*, 6843–6845.
- [6] J. Shang, Y. F. Wang, M. Chen, J. X. Dai, X. Zhou, J. Kuttner, G. Hilt, X. Shao, J. M. Gottfried, K. Wu, *Nat. Chem.* **2015**, *7*, 389–393.
- [7] X. Zhang, N. Li, G. C. Gu, C. Li, H. Wang, D. Nieckarz, P. Szabelski, Y. He, Y. Wang, C. Xie, Z. Y. Shen, J. T. Lü, H. Tang, L. M. Peng, S. M. Hou, K. Wu, Y. F. Wang, *ACS Nano* **2015**, *9*, 11909–11915.
- [8] Q. Sun, L. Cai, H. Ma, C. Yuan, W. Xu, *Chem. Commun.* **2015**, *51*, 14164–14166.
- [9] N. Li, X. Zhang, G. C. Gu, H. Wang, D. Nieckarz, P. Szabelski, Y. He, Y. Wang, J. T. Lü, H. Tang, L. M. Peng, S. M. Hou, Y. F. Wang, *Chin. Chem. Lett.* **2015**, *26*, 1198–1202.
- [10] X. Zhang, N. Li, G. C. Gu, C. Li, H. Tang, L. M. Peng, S. M. Hou, Y. F. Wang, *Chem. Commun.* **2016**, *52*, 10578–10581.
- [11] N. Li, G. C. Gu, X. Zhang, D. L. Song, Y. J. Zhang, B. K. Teo, L. M. Peng, S. M. Hou, Y. F. Wang, *Chem. Commun.* **2017**, *53*, 3469–3472.
- [12] G. C. Gu, N. Li, L. Liu, X. Zhang, Q. M. Wu, D. Nieckarz, P. Szabelski, Boon K. Teo, L. M. Peng, S. M. Hou, Y. F. Wang, *RSC Adv.* **2016**, *6*, 66548–66552.
- [13] A. R. Lahrood, N. Martsinovich, M. Lischka, J. Eichhorn, P. Szabelski, D. Nieckarz, T. Strunkus, K. Das, M. Schmittel, W. M. Heckl, M. Lackinger, *ACS Nano* **2016**, *10*, 10901–10911.
- [14] R. Sarkar, K. Guo, C. N. Moorefield, M. J. Saunders, C. Wesdemiotis, G. R. Newkome, *Angew. Chem. Int. Ed.* **2014**, *53*, 12182–12185; *Angew. Chem.* **2014**, *126*, 12378–12381.
- [15] Z. Jiang, Y. Li, M. Wang, D. Liu, J. Yuan, *Angew. Chem. Int. Ed.* **2017**, *56*, 11450–11455; *Angew. Chem.* **2017**, *129*, 11608–11613; *Angew. Chem.* **2017**, *129*, 11608–11613.
- [16] S. Karan, Y. F. Wang, R. Robles, N. Lorente, R. Berndt, *J. Am. Chem. Soc.* **2013**, *135*, 14004–14007.
- [17] A. Z. Wang, M. Zhao, *Phys. Chem. Chem. Phys.* **2015**, *17*, 21837–21844.
- [18] M. Hino, *J. Fractal Geom.* **2016**, *3*, 245–263.
- [19] J. A. Smerdon, K. M. Young, M. Lowe, S. S. Hars, T. P. Yadav, D. Hesp, V. R. Dhanak, A. P. Tsai, H. R. Sharma, R. McGrath, *Nano Lett.* **2014**, *14*, 1184–1189.
- [20] M. Z. Liu, M. G. Liu, L. M. She, Z. Q. Zha, J. L. Pan, S. C. Li, T. Li, Y. Y. He, Z. Y. Cai, J. B. Wang, Y. Zheng, X. H. Qiu, D. Y. Zhong, *Nat. Commun.* **2017**, *8*, 14924.
- [21] M. C. O'Sullivan, J. K. Sprafke, D. V. Kondratuk, C. Rinfray, T. D. W. Claridge, A. Saywell, M. O. Blunt, J. N. O'Shea, P. H. Beton, M. Malfois, H. L. Anderson, *Nature* **2011**, *469*, 72–75.
- [22] R. T. Vang, K. Honkala, S. Dahl, E. K. Vestergaard, J. Schnadt, E. Lægsgaard, B. S. Clausen, J. K. Nørskov, F. Besenbacher, *Nat. Mater.* **2005**, *4*, 160–162.
- [23] X. M. Xu, H. P. Zhong, H. M. Zhang, Y. R. Mo, Z. X. Xie, L. S. Long, L. S. Zheng, B. W. Mao, *Chem. Phys. Lett.* **2004**, *386*, 254–258.
- [24] L. Lafferentz, V. Eberhardt, C. Dri, C. Africh, G. Comelli, F. Esch, S. Hecht, L. Grill, *Nat. Chem.* **2012**, *4*, 215–220.
- [25] M. Alemani, S. Selvanathan, F. Ample, M. V. Peters, K. H. Rieder, F. Moresco, C. Joachim, S. Hecht, L. Grill, *J. Phys. Chem. C* **2008**, *112*, 10509–10514.
- [26] A. Trembulowicz, G. Ehrlich, G. Antczak, *Phys. Rev. B* **2011**, *84*, 245445.
- [27] S. Stepanow, N. Lin, D. Payer, U. Schlickum, F. Klappenberger, G. Zoppellaro, M. Ruben, H. Brune, J. V. Barth, K. Kern, *Angew. Chem. Int. Ed.* **2007**, *46*, 710–713; *Angew. Chem.* **2007**, *119*, 724–727.
- [28] C. Li, X. Zhang, Y. W. Wang, J. J. Yang, G. C. Gu, Y. J. Zhang, S. M. Hou, L. M. Peng, K. Wu, D. Nieckarz, P. Szabelski, H. Tang, Y. F. Wang, *J. Am. Chem. Soc.* **2017**, *139*, 13749–13753.
- [29] T. Chen, W. H. Yang, D. Wang, L. J. Wan, *Nat. Commun.* **2013**, *4*, 1389.
- [30] B. B. Luo, J. W. Smith, Z. X. Wu, J. Kim, Z. H. Ou, Q. Chen, *ACS Nano* **2017**, *11*, 7626–7633.
- [31] X. Zhang, G. C. Gu, Y. J. Zhang, S. M. Hou, Y. F. Wang, *Chem. Commun.* **2017**, *53*, 11826–11829.
- [32] N. Li, X. Zhang, G. C. Gu, H. Wang, D. Nieckarz, P. Szabelski, Y. He, Y. Wang, J. T. Lü, H. Tang, L. M. Peng, S. M. Hou, K. Wu, Y. F. Wang, *Chin. Chem. Lett.* **2015**, *26*, 1198–1202.

- [33] Y. H. Jiang, L. W. Liu, K. Yang, W. D. Xiao, H. J. Gao, *Chin. Phys. B* **2011**, *20*, 096401.
- [34] A. D. Yoffe, *Adv. in Phys.* **1993**, *42*, 173–262.
- [35] D. V. Melnikov, J. P. Leburton, *Phys. Rev. B* **2006**, *73*, 085320.
- [36] D. F. Ogletree, P. J. Schuck, A. F. Weber-Bargioni, N. J. Borys, S. Aloni, W. Bao, S. Barja, J. Lee, M. Melli, K. Munehikia, S. Whitelam, S. Wickenburg, *Adv. Mater.* **2015**, *27*, 5693–5719.
- [37] M. F. Crommie, C. P. Lutz, D. M. Eigler, *Science* **1993**, *262*, 218–220.
- [38] J. Kliewer, R. Berndt, E. V. Chulkov, V. M. Silkin, P. M. Echenique, S. Crampin, *Science* **2000**, *288*, 1399–1402.
- [39] Z. G. Fu, P. Zhang, Z. G. Wang, S. S. Li, *Phys. Rev. B* **2011**, *84*, 235438.
- [40] L. Vitali, P. Wahl, M. A. Schneider, K. Kern, V. M. Silkin, E. V. Chulkov, P. M. Echenique, *Surf. Sci.* **2003**, *523*, L47–L52.
- [41] C. Tournier-Colletta, B. Kierren, Y. Fagot-Revurat, D. Malterre, *Phys. Rev. Lett.* **2010**, *104*, 016802.
- [42] Y. Pennec, W. Auwáter, A. Schiffrin, A. Weber-Bargioni, A. Riemann, J. V. Barth, *Nat. Nanotechnol.* **2007**, *2*, 99–103.
- [43] A. Schiffrin, J. Reichert, W. Auwáter, G. Jahnz, Y. Pennec, A. Weber-Bargioni, V. S. Stepanyuk, L. Niebergall, P. Bruno, J. V. Barth, *Phys. Rev. B* **2008**, *78*, 035424.
- [44] J. Lobo-Checa, M. Matena, K. Müller, J. H. Dil, F. Meier, L. H. Gade, T. A. Jung, M. Stöhr, *Science* **2009**, *325*, 300–303.
- [45] S. Wang, W. Wang, L. Z. Tan, X. G. Li, Z. Shi, G. Kuang, P. N. Liu, S. G. Louie, N. Lin, *Phys. Rev. B* **2013**, *88*, 245430.
- [46] H. Wang, X. Zhang, Z. L. Jiang, Y. F. Wang, S. M. Hou, *Phys. Rev. B* **2018**, *97*, 115451.
- [47] S. N. Kempkes, M. R. Slot, S. E. Freeney, S. J. M. Zevenhuizen, D. Vanmaekelbergh, I. Swart, C. M. Smith, *Nat. Phys.* **2019**, *15*, 127–131.
- [48] D. P. Dubal, O. Ayyad, V. Ruiz, P. Gómez-Romero, *Chem. Soc. Rev.* **2015**, *44*, 1777–1790.
- [49] J. A. Fan, W. H. Yeo, Y. W. Su, Y. Hattori, W. Lee, S. Y. Jung, Y. H. Zhang, Z. Liu, H. Cheng, L. Falgout, M. Bajema, T. Coleman, D. Gregoire, R. J. Larsen, Y. Huang, J. A. Rogers, *Nat. Commun.* **2014**, *5*, 3266.
- [50] F. D. Nicola, N. S. Puthiya Purayil, D. Spirito, M. Miscuglio, F. Tantussi, A. Tomadin, F. D. Angelis, M. Polini, R. Krahne, V. Pellegrini, *ACS Photonics* **2018**, *5*, 2418–2425.
- [51] M. Brzezińska, A. M. Cook, T. Neupert, *Phys. Rev. B* **2018**, *98*, 205116.
- [52] P. W. K Rothemund, N. Papadakis, E. Winfree, *PLoS Biol.* **2004**, *2*, 2041–2053.

Manuscript received: March 15, 2019

Revised manuscript received: May 24, 2019

Version of record online: July 10, 2019